Proceedings World Geothermal Congress 2023
Beijing, China, April 17 – 21, 2023

Thermal performance comparison and sensitivity analysis of elliptical and conventional single U-tube borehole heat exchangers: Numerical approach

Basher Hassan Al-Kbodi[1,2], Taha Rajeh[1], Yang Li[1,*], Jun Zhao[1,*]

[1]Key Laboratory of Efficient Utilization of Low and Medium Grade Energy (Tianjin University), Ministry of Education of China, Tianjin 300350, China

[2]Alsaeed Faculty for Engineering and Information Technology, Taiz University, Taiz, Yemen
E-mail address: zhaojun@tju.edu.cn (J. Zhao), liyangtju@tju.edu.cn (Y. Li)

Keywords: Ground-coupled heat pump; borehole heat exchanger; heat transfer rate; numerical simulation; single U-tube.

ABSTRACT

Borehole heat exchangers (BHEs) are critical components of ground-coupled heat pump (GCHP) systems, and their thermal performance is consequently significant for GCHP system design and operation. This paper investigates the heat transfer characteristics of an elliptical BHE and compares it to conventional single U-tube BHE. All numerical simulations are carried out using a 3D numerical model, and all of the models under consideration have the same heat transfer area. The experimental data is used to validate the numerical simulations. The sensitivity analysis was carried out and the effects of several operating and design parameters on heat exchange were investigated. The influence of the elliptical U-tube geometry parameters on the BHE's thermal performance is evaluated using the shape's slope angle and shape's factor. The results show that the average and maximum heat transfer rate of the elliptical BHE can be raised by 11.55% and 22.09% compared with the conventional single BHE. Furthermore, the sensitivity analysis demonstrated that flow rate, BHE materials, BHE depth, and cross-section tube area have the most influence on elliptical tube BHE. These findings could be used as a guideline for future BHE research, particularly in terms of heat transfer and pressure drop performance perspectives.

1. INTRODUCTION

Studying ground-coupled heat pump (GCHP) articles and studies reveals the development of fundamental knowledge over the past two decades on its structure and operation, leading to a better understanding of these green technologie's dynamic and thermal effectiveness. The borehole heat exchanger (BHE) is the heart of the GCHP; proper BHE design leads to improved thermal performance (Florides et al., 2008; Gehlin, 2016). Furthermore, nearly 51% of the primary investment of the GCHP system is comprised of the price of drilling the borehole and purchasing grout material (Huang and Mauerhofer, 2016; Lu et al., 2017a, 2017b). In addition, (Wang et al., 2018) demonstrated that the borehole depth must be at least 70 meters to ensure greater long-term consumption of energy. Subsequently, these results demonstrated that the depth and number of boreholes are the key factors in the overall cost of GCHP systems (Robert and Gosselin, 2014).

Indeed, researchers are currently focusing on enhancing the thermal efficiency of BHE in order to reduce the depth of the borehole and, subsequently, its costs of installation and drilling. Altering the heat exchanger's design and shape can improve heat transfer and decrease borehole depth. Consequently, various concepts are suggested and developed within this context. (Zhang et al., 2015) investigated the differences between double and single U-tubes in a similar borehole size. The study showed that using a double U-tube design led to a reduction of 17.14% in the depth of the borehole. In addition, According to (Florides et al., 2013) in their research, they found that a double U-tube circular shape with a parallel configuration was more efficient by 26-29% compared to a singular U-tube circular shape. However, the cost of construction was also found to be 22-29% higher. (Aydin and Sisman, 2015) experimentally evaluated the performance of various configurations of U-tubes, it was found that using two or three U-tubes resulted in a 14% and 25% improvement, respectively, when compared to using a single U-tube. However, using four or five U-tubes resulted in only slight improvement. In addition, (Liu et al., 2015) presented a BHE with one outlet pipe (diameter: 32 mm) and three inlet pipes (diameter: 25 mm). Compared to a single pipe, it reduced the thermal resistance of the borehole by 59.16%. (Zarrella et al., 2013a) discovered that the helical heat exchanger outperformed the double U-tube cross-section by 33%. However, a larger borehole diameter, 2–4 times the typical diameter, is typically required for helical BHE and multi-tube BHE (Aydin and Sisman, 2015; Zarrella et al., 2013b). In addition, a support structure is also needed to maintain its shape, which may make construction more difficult (Aydin and Sisman, 2015; Saeidi et al., 2018; Zarrella et al., 2013b). The helical BHE and multi-tube BHE are found to be particularly well suited for use in energy piles (Zhao et al., 2016).

Recently, different novel shapes of single BHEs have been investigated, (Serageldin et al., 2018) proposed a new pipe design with an oval shape. According to their research, this new shape of oval BHE can reduce the internal heat resistance of the borehole and enhance the heat transfer efficiency by 18.47%. These improvements make it a suitable option for high-density areas such as urban areas. (Jahanbin, 2020) proposed the idea of utilizing an elliptical shaped buried pipe and evaluated how variations in the elliptical geometry affected the thermal resistance. Compared to conventional circular cross-section pipes, the elliptical cross-section reduced heat resistance in boreholes by approximately 17 %. As the elliptical dimensionless factor increases, this reduction increases. (Zhou et al., 2021) examined the heat exchange effectivness of the BHE with various shapes of U-tube BHEs (circle, oval, elliptical, sector, and semicircle). According to their findings, altering the U-cross-sectional tube's shape can improve the heat transfer of BHEs. Their research was conducted with uniform shank spacing and cross-sectional area. Compared to the circular shape, the heat transfer efficiencies of the oval cross-section, elliptical cross-section, sector cross-section, and semicircle cross-section increased by 19.1 %, 13.0 %, 14.8%, and 9.4 %, respectively. The current state of the literature shows few studies on the tube-shaped configurations of a single U-tube BHE. However, a detailed key design and operating parameters using the heat flux as the evaluation parameter of the heat transfer performance, as well as a comprehensive sensitivity analysis comparing elliptical tube-shaped BHE to circular tube-shaped BHE, have not been introduced in the literature.

On the basis of the previously presented studies, we implemented a three-dimensional, non-steady-state numerical model validated by experimental data from the literature. The adopted numerical model accurately captures the long-term and short-term behavior of

the proposed BHEs and permits an analysis of the changes in heat exchange performance throughout the BHEs. This research aims to investigate the heat exchange performance of the elliptical cross-section BHE compared to the circular cross-section BHE using the BHE heat flux as an evaluation parameter by providing an intensive comparison including mass flow rate, BHE materials, BHE length, backfill thermal conductivity, soil thermal conductivity, shank spacing, and alternative geometrical parameters. In addition, this paper performed a sensitivity analysis. The main findings of this paper could help with the design and development of BHEs.

2. MODELS AND BOUNDARY CONDITIONS

In this study, ANSYS Fluent commercial software was used to build and analyze a three-dimensional numerical model of a single U-tube BHE. The studied BHE configurations in this paper are the circular U-tube BHE and elliptical U-tube BHE cross-sections. Figure 1 shows a drawing of the BHE shapes for both models. As shown in Figure 1, the 3D-numerical model was separated into four sections: the soil exterior to the borehole, the soil filling the borehole, the tube, and the working fluid. Table 1 shows the geometric and operating parameters. Maintaining comparable borehole diameter, shank spacing, pipe thickness, and cross-sectional area would contribute to a more reliable comparison study in order to evaluate the impact of cross-sectional shape on the heat exchange performance of BHEs. The flow field's complexity substantially affects calculation time and convergence speed in the bottom section of various BHE configurations. It is excluded from the geometric model because it is rather tiny in comparison to the rest of BHE. We utilized a user-defined function (UDF) to connect the inlet and outlet tubes. The boundary conditions are presented in Table 2, and the material parameters are illustrated in Table 3. The BHE runs in cooling mode 24 h a day, with the inlet temperature set to 30 ℃. For the outlet and inlet boundary conditions, the pressure outlet and mass flow rate inlet are selected, respectively. To simulate the turbulent fluid flow within the U-tube, we utilized the k-epsilon model and the SIMPLE algorithm to account for the velocity and pressure condition. In the simulation, a time step size of 60 s was used. The convergence of numerical simulations was achieved every time step for all simulated cases in the present work.

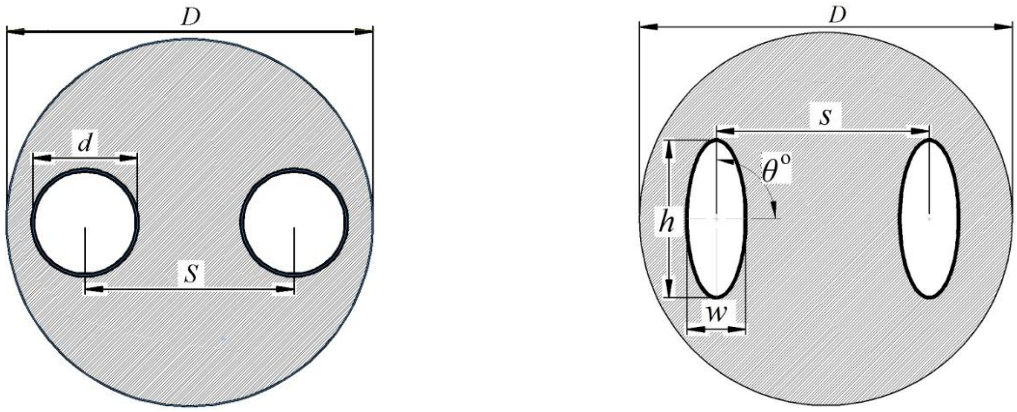

(a) (b)

Figure 1. Cross section of the studies tube shapes. (a) Circular shape (b) Elliptical shape.

Table 1. Parameter description of the cross-section and studied factors.

Parameter	Value (unit)	Reference value
Soil Diameter	8 (m)	8
Area, A	531, 830, 1018(mm^2)	830
Circular	Diameter: 32.6 (mm); angle: 360˚	32.6
Elliptical	axis h: 52, 60, 68 (mm); short axis w: 20.32, 17.6, 15.54 (mm)	h: 60, w: 17.6
Flow rate, M	0.1, 0.2, 0,4, 0.6, 0.8, 1.2 (kg/s)	0.6
Depth, H	50, 100, 120, 150 (m)	120
Shank spacing, S	70, 90, 110 (mm)	90
Tube thermal conductivity, λ_{BHE}	0.13, 0.4, 15.5, 202.4 (W/m·K)	0.4
Soil thermal conductivity, λ_s	1.26, 1.39, 1.5, 1.7 (W/m·K)	1.5
Backfill thermal conductivity, λ_{bf}	1, 1.5, 2 (W/m·K)	1.5
Shape factor, γ	0.44, 0.54, 0.63 (%)	0.54
Inclined angle, θ	45˚, 90˚, 180˚	90˚
Borehole diameter, D	152 (mm)	152

Table 2. The boundary condition.

BHE structure	Boundary condition	
Fluid	Inlet	30 ℃, M = 0.6 kg/s
	Outlet	P=0 Pa (gauge)
Solid	Top Surface	Adiabatic
	Bottom surface	Adiabatic
	Outer soil wall	Constant vertical temperature distribution

Table 3 Material physical properties.

Part	ρ (kg/m^3)	c_p (J/(kg·K))	λ (W/m·K)	μ (Pa·s)
soil	1220	2070	1.5	-
BHE	1000	1824	0.4	-
Water	1000	4180	0.60	0.001

2.1 Assumptions

1. The working fluid, backfill materials, soil, and BHE have constant and homogeneous physical properties.
2. The temperature distribution is equal to the initial temperature for the radial boundary of the soil.
3. Groundwater flow is overlooked.
4. Natural convection is overlooked.

2.2 Initial conditions

The initial soil temperatures for heating and cooling simulations are regressed from measured data by the Institute for the Exploration and Development of Geothermal Resources in Tianjin. The equations are presented in our prior work (Li et al., 2020).

2.3 Study Factors

2.3.1 Heat Flux per Unit Length

The working fluid's outlet and inlet temperatures are calculated to determine the BHE's heat flux per unit length (q). Eq.(2) is used to compute the heat flux per unit length:

$$q = \frac{Q}{H} = Mc_p(T_{in} - T_{out}) / H \tag{1}$$

where Q represents heat exchange rate (kg/s), H represents depth (m), M represents flow rate (kg/s), c_p represents specific heat capacity (J/kg K), and T_{in} and T_{out} are inlet and outlet working fluid temperature (K), respectively.

2.3.2 Shape Factor

For a valid comparison between the heat transfer performance of circular BHE cross-section and that of elliptical BHE cross-section, the cross-section area of the elliptical shape was set to be the same as that of the circular shape. To meet this criterion, the following shape factor γ is presented as follows (Jahanbin, 2020):

$$\gamma = \frac{a-b}{a+b} \tag{2}$$

where b and a represent the ellipse's semi-minor axes and semi-major, respectively. We evaluated three different elliptical U-tube shapes, as shown in Table 1. Each ellipse has an area A of 830 mm^2, which is the same area as the typical circular U-tube.

3. MESH AND MODEL VALIDATION

Since the shapes of studied BHE configurations are identical, the proposed model was divided into a 1/2 symmetric model. Figure 2 depicts the horizontal grid of the three-dimensional model. The meshes were all well-organized, with nearly 99.95% having an EquiSize skew of less than 0.45. The heat flux per unit length is computed as independence tests In order to enhance calculation accuracy while keeping calculation effectiveness as shown in Table.4. The reference parameters, as shown in Table 1 and the conditions for the mesh tests are illustrated in Table 2 and Table 3. According to the test results, the optimal mesh element for circular BHE and elliptical BHE is 466320 and 622200, respectively. The maximum difference in the heat flux for various mesh sizes is less than 0.046%. Convergence was achieved in every time step of the simulations presented in this paper. These numerical simulations are validated by an experiment conducted by (Jalaluddin et al., 2011). (see Figure 3). The validation results demonstrated that the numerical model and the experimental data are in excellent agreement with an average absolute error for the outlet temperature of 0.21℃, which validates the reliability of the adopted numerical model.

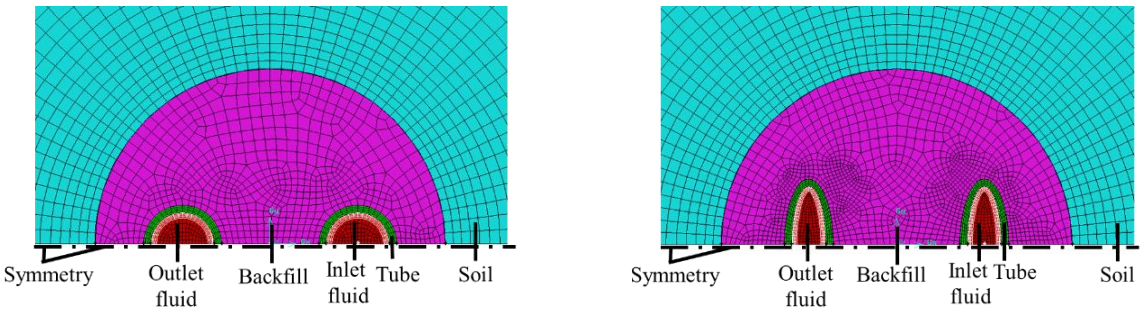

(a) (b)

Figure 2. The 3-D model's horizontal grid: (a) circular shape (b) Elliptical shape.

Table 4 Mesh independence [M = 0.6 kg/s and T_{in} = 30 ℃]

circular BHE		Elliptical BHE	
Number of element	Change ratio of Δq	Number of element	Change ratio of Δq
116580	0.408%	155550	0.177%
233160	0.097%	311100	0.064%
466320	0.046%	622200	0.013%
932640	-	1244400	-

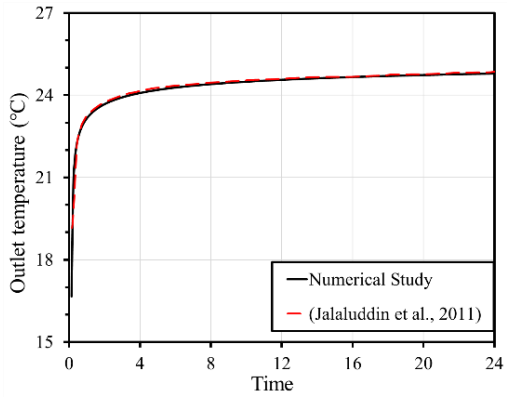

Figure 3. Validation of the numerical model to (Jalaluddin et al., 2011).

4. RESULTS AND DISCUSSION

The effect of crucial operational and design parameters on the heat flux of proposed configurations was studied. Additionally, to M and the thermal conductivity of BHE materials λ_{BHE}, the following variables were considered: BHE depth H, the thermal conductivity of backfill materials λ_{bf}, area of heat carrier fluid A, shanking space S, the thermal conductivity of soil λ_s, pipe wall thickness t, shape factor γ, and slope angle θ. The parameters of the control case reference were listed in Table 1, and the remaining parameters were similar to those in Table 3.

4.1 HIGH SENSITIVE PARAMETERS

4.1.1 Flow rate

The heat flux per unit length q is calculated based on equation (1), and the results of the proposed design configurations are shown in Figure 4. q grows significantly as the flow rate increases, as shown in Figure 4(a). The elliptical BHE cross-section exchanges more heat than the circular BHE cross-section because the elliptical BHE cross-section has a greater heat transfer area than circular BHE cross-section; the larger heat transfer area (i.e., the outer surface of the tube in contact with the soil). Figure 4(b) illustrates the increasing ratio of q for elliptical BHE compared to circular BHE versus operating time with varying flow rates. It is worth to mentioning that the increasing ratio of $q_{elliptical}$ compared with $q_{circular}$ is the highest at the beginning of the operation. For example, when M is 0.6 kg/s, the growth ratio is up to 15.69% because heat exchange between the heat carrier fluid, backfill material, and surrounding soil has not yet occurred during the early stages of the cooling process, and the temperature difference between the inlet and outlet water is particularly high, especially before one hour. In the latter stages of the cooling process, greater heat transfer occurs, resulting in a rise in T_{out} of the water; hence, the temperature change decreases and becomes almost constant after 12 hours.

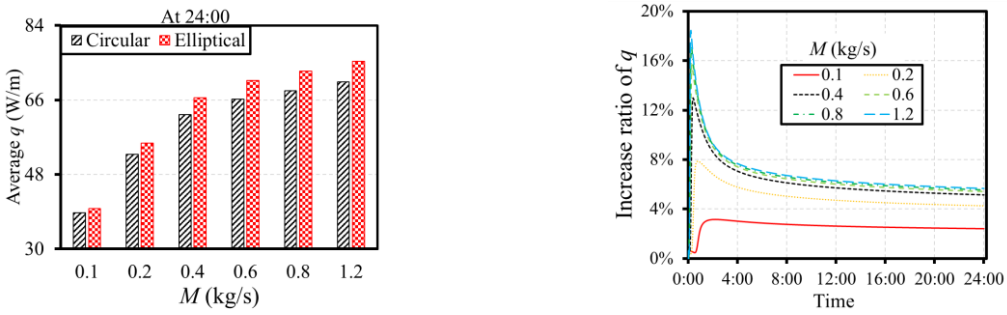

Figure 4 Heat flux for proposed BHE models: (a) Average heat flux at 24 h (b) Increasing ratio of q.

4.1.2 Thermal conductivity of pipe

In this section, λ_{BHE} (W/m·K) values of 0.13, 0.40, 1.5, 15.50, and 202.4 were chosen, which correspond to the thermal conductivity of polyvinyl chloride, polyethylene, soil, stainless steel, and aluminum, respectively. The variation in volumetric heat capacity was overlooked. Figure 5(a) depicts the average q for various λ_{BHE} values relative to circular BHE at 24:00 h. As λ_{BHE} grows, q always increases as well. When the thermal conductivity of the pipe exceeds 15.5 W/m·K, the increase becomes limited (Cao et al., 2017; Tang and Nowamooz, 2019). For a given λ_{BHE}, since the elliptical cross-section BHE has a higher heat exchange area, the design with the larger heat exchange area (the outer surface of the tube in contact with the soil) compared to circular cross-section BHE, q of elliptical cross-section BHE is higher than q of circular cross-section BHE. Figure 5(b) shows the increasing ratio of q versus operating time under different λ_{BHE} compared to circular BHE; the highest increase ratio of q of the elliptical shape compared to the circular shape can be detected at PVC because of the soil thermal resistance. The average and maximum q of the elliptical BHE cross-section increased by 11.55% and 22.09% in contrast to the circular BHE cross-section when λ_{BHE} equals 0.13 W/m·K.

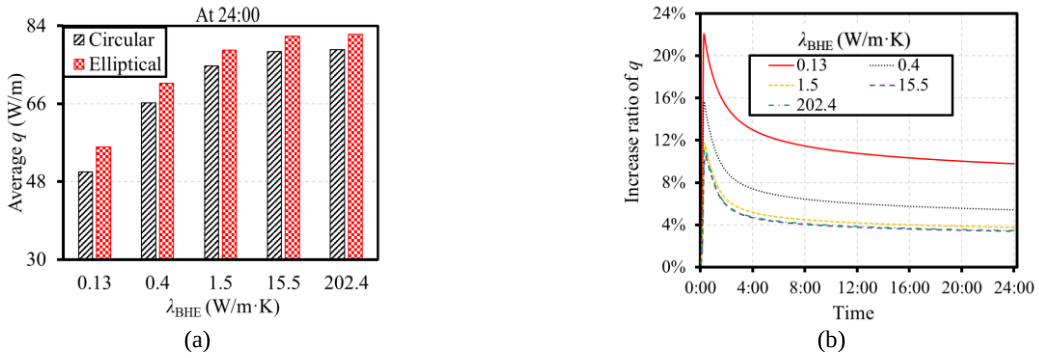

Figure 5 Simulation results at various λ_{BHE}: (a) Average heat flux at 24 h (b) Increasing ratio of q.

4.1.3 Depth of pipe

According to an ASHRAE guidebook (Kavanaugh and Rafferty, 2014), three common BHE depths H (m) were chosen for evaluation: 50, 90, and 150. The overall rate of change of q at various depths is presented in Table 5. At different durations, q drops with a rise in H, which is a result of the rapidly increasing thermal circuit. However, at the beginning of the operation, the average q reduces significantly, as observed in previous study (Li et al., 2014). The best q of elliptical BHE cross-section compared to the circular BHE cross-section can be detected at 50 m depth, and the average increasing ratio of $q_{elliptical}$ at 1, 6, and 24 h compared to circular BHE cross-section are 12.45, 9.82, and 7.57 %, respectively.

4.1.4 Backfill thermal conductivity

Three λ_{bf} (W/m·K) were chosen: 1, 2, and 3.2 based on the Tianjin city (Ruan et al., 2017). The variation in volumetric heat capacity was overlooked. Table 5 displays the average ratio of change of q at various timeframes. In general, for the studied design configurations, as λ_{bf} increases, q increases, and the average change ratio of q compared to the standard case decreases. However, when λ_{bf} increases, the increasing ratio of q compare to circular cross-section will decrease. At 24 hours, the values of the growing ratio of $q_{elliptical}$ for λ_{bf} = 1, 2, and 3.2 W/(m·K) compared to $q_{circular}$ are 7.46, 6.51, and 6.03 %, respectively.

4.1.5 Area of the tube cross-section

For shallow BHEs, the tube shape area improves the thermal efficiency of the BHEs (Sandler et al., 2017). Additionally to the standard tube cross-section area in this study of 830 mm^2, two additional tube cross-section areas A (mm^2) were chosen: 530 and 1018 . In order to ensure a proper comparison, the thickness of the circular and elliptical tubes, as well as the shape factor (γ = 54%) of the elliptical tube, are held constant during the study of the tube cross-section area effect. Table 5 shows the average ratio of change of q for the two studied tube shape areas at various timeframes. For the two studied BHEs tube-shaped, increasing A will increase q. For instance, over 24 hours, when A = 530 and 1018 mm^2, the increase ratio in average $q_{elliptical}$ compared to $q_{circular}$ is 6.36 and 6.89 %, respectively.

4.2 LESS SENSITIVE PARAMETERS

4.2.1 Shanking space

Two shank space S (mm) were selected for comparison: 70, and 90, besides the standard case 90. The average change ratio of q at various S throughout the selected periods is presented in Table 5. The shank space affects the heat exchange area of the BHEs, and increasing the shank space improves the thermal performance of the BHEs (Tang and Nowamooz, 2019). As S increases, q increases, and the average change ratio of q compared to the standard case increase as shank space increases due to the short-circuit phenomena. At 24 hours, the values of the growing ratio of $q_{\text{elliptical}}$ for S = 70 and 110 (mm) compared to q_{circular} are 6.68% and 6.72%.

4.2.2 Soil thermal conductivity

Two typical Tianjin soil thermal conductivity λ_s (W/m·K) values, 1.26 and 1.7, were chosen (Ruan et al., 2017). Variation in the volumetric heat capacity was overlooked. Table 5 presents the average ratio of change of q of the studied BHE configurations under various duration for specified λ_s. The change ratio of q of the studied BHE configurations increases with increasing λ_s. However, λ_s has a minor influence during the early stages of operation on the proposed BHE configurations. As operating time increases, the influence of λ_s increases because of the increased thermal resistance of the surrounding side. Also, when λ_s increases the increasing ratio of $q_{\text{elliptical}}$ compared with circular cross-section will increases too, for instance, over 24 hours when λ_s= 1.26 and 1.7 W/m·K, the increase ratio in average $q_{\text{elliptical}}$ compared to q_{circular} are 6.52 and 7.08 %.

4.2.3 Pipe thickness

Two pipe thickness t (mm) were chosen for evaluation: 2.5, and 4.7. The average change ratio of q at various thicknesses values throughout the selected operation periods is presented in Table 5. The results demonstrate that the change ratio of q of the proposed BHE designs reduces uniformly with the wall thickness of the U-pipe because the thinner U-pipe wall has a lower thermal resistance(Tang and Nowamooz, 2019). The best q of elliptical BHE cross-section compared to the circular BHE cross-section can be detected at 4.7 mm pipe thickness with an average increasing ratio over 24 h is 6.98%.

4.2.4 Shape factor

The Shape factor γ is calculated by using equation (2), and the results of the elliptical BHE cross-section for the average ratio of change of q is presented in Table 5. Two γ (%) were selected: 44, and 63, besides the standard case 54. The results show that the increased value of γ produces an upper change ratio of q of the elliptical BHE configuration. In addition, the increasing ratio of $q_{\text{elliptical}}$ compared to q_{circular} is an increasing function of γ; an upper value of γ produces to a higher increase ratio of $q_{\text{elliptical}}$ compared to q_{circular}. For example, over 24 hours, when γ = 44%, provides increment percentage is 3.98%, while when γ = 63%, the increment percentage increases to 9.69%, and this scenario is identical to that described by (Jahanbin, 2020). The results suggest that a U-tube with an elliptical shape, irrespective of shape factor γ, has a high potential to improve the thermal efficiency of the BHE in GCHP systems. Actually, the elliptical BHE shape has a greater tube surface area than the circular BHE shape with the same cross-sectional area, and the elliptical tube surface area increases with increasing γ.

4.2.5 Inclined angle

Two θ (˚) were selected: 45, and 180, besides the standard case 90. Table 5 presents the average change ratio of q of the elliptical BHE cross-section under different duration for specified θ. The results show that the θ has a slight influence on the BHE performance.

Table 5 Average change ratio of q under the key design and operating parameters.

Parameter	Unit	Value	Change ratio of q under various timeframe					
			1 h		6 h		24 h	
			Circular	Elliptical	Circular	Elliptical	Circular	Elliptical
L	m	50	22.18%	25.34%	14.96%	16.23%	12.20%	12.95%
		90	10.01%	10.99%	6.57%	7.00%	5.30%	5.56%
		150	-9.11%	-9.74%	-6.53%	-6.85%	-5.50%	-5.71%
λ_{bf}	W/m·K	1	-7.46%	-7.41%	-11.74%	-11.32%	-11.45%	-10.94%
		2	4.85%	4.89%	7.56%	7.27%	7.07%	6.71%
		3.2	11.96%	11.92%	18.09%	17.34%	16.51%	15.61%
A	mm^2	531	-10.69%	-10.72%	-6.60%	-7.11%	-4.80%	-5.24%
		1018	6.93%	6.57%	4.53%	4.52%	3.31%	3.34%
S	mm	70	-4.01%	-4.03%	-5.86%	-6.11%	-5.49%	-5.65%
		110	2.55%	1.94%	4.77%	4.56%	4.73%	4.60%
λ_s	W/m·K	1.26	-2.28%	-2.19%	-4.08%	-2.26%	-6.59%	-6.89%
		1.7	2.23%	2.13%	1.50%	3.60%	5.31%	5.53%
t	mm	2.5	5.04%	4.53%	4.48%	3.69%	3.62%	2.90%
		4.7	-3.27%	-3.49%	-3.10%	-3.06%	-2.58%	-2.47%
γ	%	44	-	-3.84%	-	-3.37%	-	-2.69%
		63	-	3.71%	-	3.29%	-	2.65%
θ	˚	45	-	-0.86%	-	-0.10%	-	-0.06%
		180	-	-2.45%	-	-0.61%	-	-0.45%

4.3 SENSITIVITY ANALYSIS

A sensitivity analysis was performed using the above stated parameters. The sensitivity analysis includes three operating timeframes: 1 hour, 6 hours, and 24 hours because the influence of long-term and short-term operations on q differs with the time. Figure 6(a, b) shows the change ratio of average q by a tornado diagram over each timeframe for the two studied BHE design configurations. The greatest sensitive parameter is M, followed by λ_{BHE}, L, λ_{bf}, and A. The effect of M, λ_{BHE}, L, and A is more significant at the beginning of the operation time. Nevertheless, the impact of the parameters λ_s, S, k, γ, and θ is limited. The sensitivity analysis indicates that for the circular BHE cross-section and elliptical BHE cross-section applications, the flow rate, BHE materials, BHE depths, heat carrier fluid area, and backfill materials must be carefully designed. For the circular BHE cross-section, previous studies (Han and Yu, 2016; Sandler et al., 2017; Tang and Nowamooz, 2019) also revealed that M, λ_{BHE}, L, λ_{bf}, and A were the most influential parameters, which were symmetric to the findings of the current investigation. As a result, the sensitivity analysis demonstrated that flow rate, BHE materials, BHE depth, and cross-section tube area have a greater influence on elliptical tube BHE than circular tube BHE.

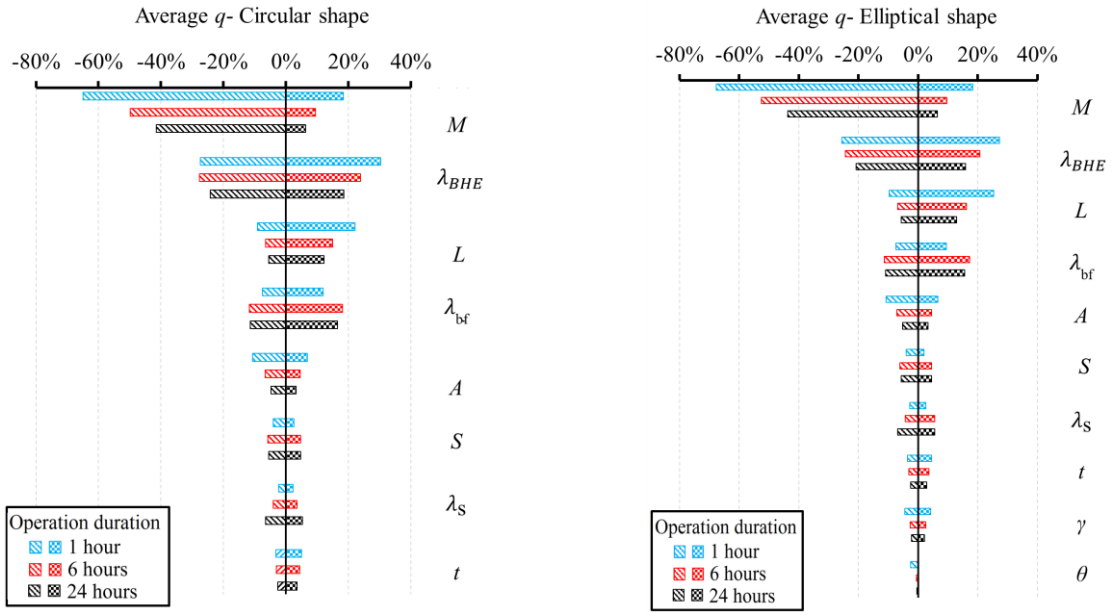

Figure 6 Sensitivity analysis for different operating durations: (a) Circle cross-section tube BHE (b) Elliptical cross-section tube BHE.

5. CONCLUSIONS

This research studies and compares the heat transfer characteristics of an elliptical BHE to a typical single U-tube BHE. All numerical simulations are performed using a 3D numerical model, and the proposed configurations have the same heat exchange area. The numerical simulations are validated using experimental data from the literature. A sensitivity analysis was conducted to determine the influence of various main design and operating parameters on the BHE heat transfer performance. The main findings are as follows:

- In all studied parameters, employing the elliptical cross-section could increase the heat transfer rate compared with a circular cross-section.
- The upper values of the factor of shape lead to a higher value of heat flux.
- In contrast to conventional single BHE, the average and maximum heat exchange rate of the elliptical BHE raised by 11.55% and 22.09%, respectively.
- The flow rate, BHE materials, BHE depths, heat carrier fluid area, and backfill materials are the most sensitive parameters.

6. REFERENCES

Aydin M, Sisman A.: Experimental and computational investigation of multi U-tube boreholes, *Appl Energy*, **145**, (2015),163–71.

Cao SJ, Kong XR, Deng Y, Zhang W, Yang L, Ye ZP.: Investigation on thermal performance of steel heat exchanger for ground source heat pump systems using full-scale experiments and numerical simulations, *Appl. Therm. Eng.*, **115**, (2017), 91–8.

Florides, G., Kalogirou, S.: First in situ determination of the thermal performance of a U-pipe borehole heat exchanger, in Cyprus, *Appl. Therm. Eng.*, **28**, (2008), 157–163.

Florides GA, Christodoulides P, Pouloupatis P.: Single and double U-tube ground heat exchangers in multiple-layer substrates, *Appl Energy*, **102**, (2013), 364–73.

Gehlin, S.: Borehole thermal energy storage, *Advances in Ground-Source Heat Pump Systems*, (2016), 295-327.

Han, C., Yu, X.: Sensitivity analysis of a vertical geothermal heat pump system, *Appl. Energy*, **170**, (2016), 148–160.

Huang, B., Mauerhofer, V.: Life cycle sustainability assessment of ground source heat pump in Shanghai, *China. J. Clean. Prod.* **119**, (2016), 207–214.

Jahanbin, A.:Thermal performance of the vertical ground heat exchanger with a novel elliptical single U-tube, *Geothermics*, 86, (2020), 101804.

Jalaluddin, Miyara, A., Tsubaki, K., Inoue, S., Yoshida, K.: Experimental study of several types of ground heat exchanger using a steel pile foundation, *Renew. Energy*, **36**, (2011), 764–771.

Kavanaugh, S.P., Rafferty, K.D.: Geothermal heating and cooling: design of groundsource heat pump systems, *ASHRAE*, (2014).

Li, Y., Ma, L., Xu, W., Zhu, Q., Li, W., Zhao, J., Zhu, J.: Multi-external-chamber coaxial borehole heat exchanger: Dynamic heat transfer and energy consumption analysis, *Energy Convers. Manag.*, **207**, (2020), 112519.

Li, Y., Mao, J., Geng, S., Han, X., Zhang, H.: Evaluation of thermal short-circuiting and influence on thermal response test for borehole heat exchanger, *Geothermics*, **50**, (2014), 136–147.

Liu, Y., Zhang, Y., Gong, S., Wang, Z., Zhang, H.: Analysis on the Performance of Ground Heat Exchangers in Ground Source Heat Pump Systems based on Heat Transfer Enhancements, *Procedia Eng.*, **121**, (2015), 19–26.

Lu, Q., Narsilio, G.A., Aditya, G.R., Johnston, I.W.: Economic analysis of vertical ground source heat pump systems in Melbourne, *Energy*, **125**, (2017a), 107–117.

Lu, Q., Narsilio, G.A., Aditya, G.R., Johnston, I.W.: Cost and performance data for residential buildings fitted with GSHP systems in Melbourne Australia, *Data Br.*, **12**, (2017b), 9–12.

Robert, F., Gosselin, L.: New methodology to design ground coupled heat pump systems based on total cost minimization, *Appl. Therm. Eng.*, **62**, (2014), 481–491.

Ruan, C., Feng, S.: An analysis of the characteristics of thermal physical properties and their influencing factors in the Tianjin area, *Hydrogeol Eng Geol*, **44, (**2017), 158–63 [in Chinese].

Saeidi, R., Noorollahi, Y., Esfahanian, V.: Numerical simulation of a novel spiral type ground heat exchanger for enhancing heat transfer performance of geothermal heat pump, *Energy Convers. Manag.*, **168**, (2018), 296–307.

Sandler, S., Zajaczkowski, B., Bialko, B., Malecha, Z.M.: Evaluation of the impact of the thermal shunt effect on the U-pipe ground borehole heat exchanger performance, *Geothermics*, **65**, (2017), 244–254.

Serageldin, A.A., Sakata, Y., Katsura, T., Nagano, K.: Thermo-hydraulic performance of the U-tube borehole heat exchanger with a novel oval cross-section: Numerical approach, *Energy Convers. Manag.*, **177**, (2018), 406–415.

Tang, F., Nowamooz, H.: Factors influencing the performance of shallow Borehole Heat Exchanger, *Energy Convers. Manag.*, **181**, (2019), 571–583

Wang, X., Wang, Y., Wang, Z., Liu, Y., Zhu, Y., Chen, H.: Simulation-based analysis of a ground source heat pump system using super-long flexible heat pipes coupled borehole heat exchanger during heating season, *Energy Convers. Manag.*, **164**, (2018), 132–143.

Zarrella, A., Capozza, A., De Carli, M.: Analysis of short helical and double U-tube borehole heat exchangers: A simulation-based comparison, *Appl. Energy*, **112**, (2013a), 358–370.

Zarrella, A., De Carli, M., Galgaro, A.: Thermal performance of two types of energy foundation pile: Helical pipe and triple U-tube. Appl, *Therm. Eng.*, **61**, (2013b), 301–310.

Zhang, W., Yang, H., Lu, L., Fang, Z.: Investigation on influential factors of engineering design of geothermal heat exchangers, *Appl. Therm. Eng.*, **84**, (2015), 310–319.

Zhao, J., Li, Y., Wang, J.: A Review on Heat Transfer Enhancement of Borehole Heat Exchanger, *Energy Procedia*, **104**, (2016), 413–418.

Zhou, A., Huang, X., Wang, W., Jiang, P., Li, X.: Thermo-hydraulic performance of u-tube borehole heat exchanger with different cross-sections, *Sustain.*, **13**, (2021), 1–20.

.